Atmos. Chem. Phys. Discuss., doi:10.5194/acp-2016-1096, 2016
Manuscript under review for journal Atmos. Chem. Phys.
Published: 6 December 2016

Atmospheric Chemistry and Physics Discussions

Size distribution and source of black carbon aerosol in urban Beijing during winter haze episodes

Yunfei Wu[1,*], Xiaojia Wang[1], Jun Tao[2], Rujin Huang[3], Ping Tian[4], Junji Cao[3], Leiming Zhang[5], Kin-Fai Ho[6], Renjian Zhang[1,*]

1 Key Laboratory of Regional Climate-Environment for Temperate East Asia, Institute of Atmospheric Physics, Chinese Academy of Sciences, Beijing, China
2 South China Institute of Environmental Sciences, Ministry of Environmental Protection, Guangzhou, China
3 Key Laboratory of Aerosol Chemistry and Physics, Institute of Earth Environment, Chinese Academy of Sciences, Xi'an, China
4 Beijing Weather Modification Office, Beijing, China
5 Air Quality Research Division, Science Technology Branch, Environment Canada, Toronto, Canada
6 The Jockey Club School of Public Health and Primary Care, The Chinese University of Hong Kong, Hong Kong, China

* Correspondence to: Yunfei Wu (wuyf@mail.iap.ac.cn) and Renjian Zhang (zrj@mail.iap.ac.cn)

Atmos. Chem. Phys. Discuss., doi:10.5194/acp-2016-1096, 2016
Manuscript under review for journal Atmos. Chem. Phys.
Published: 6 December 2016

Atmospheric Chemistry and Physics Discussions

Abstract

Black carbon (BC) plays an important role in the climate and environment due to its light absorption, which is greatly dependent on its physicochemical properties including morphology, size and mixing state. The size distribution of the refractory BC (rBC) in urban Beijing during the late winter in 2014 was revealed by measurements obtained using a single particle soot photometer (SP2), when the hazes occurred frequently. By assuming void-free rBC with a density of 1.8 g cm^{-3}, the mass of the rBC showed an approximately lognormal distribution as a function of the volume-equivalent diameter (*VED*), for which there was a peak diameter of 213 nm. This size distribution agreed well with those observed in other urban areas of China. Larger *VED* values of the rBC were observed during polluted periods than on clean days, implying an alteration in the rBC sources, as the mass-size of the rBC from a certain source varied little once it was emitted into the atmosphere. The potential source contribution functions showed that air masses from the south to east of the observation site brought a higher rBC loading with more thick coatings and larger core sizes. The mean *VED* of the rBC presented a significant linear correlation with the number fraction of thickly coated rBC; the *VED* of the entirely externally mixed rBC was inferred as the *y*-intercept of the linear regression. This *VED*, with a value of ~150 nm, was considered as the typical mean *VED* of the rBC from local traffic sources in this study. Accordingly, the contribution of the local traffic to the rBC was estimated based on reasonable assumptions. Local traffic contributed 35 to 100% of the hourly rBC mass concentration with a mean of 59%, during this campaign. A lower local traffic contribution was observed during polluted periods, suggesting increasing contributions of other sources (e.g., coal combustion/biomass burning) to the rBC. The heavy pollution in Beijing was greatly influenced by other sources in addition to the local traffic.

Keywords: black carbon aerosol, size distribution, source, haze

Atmos. Chem. Phys. Discuss., doi:10.5194/acp-2016-1096, 2016
Manuscript under review for journal Atmos. Chem. Phys.
Published: 6 December 2016

Atmospheric Chemistry and Physics Discussions

1 Introduction

Black carbon (BC), the major light-absorbing component in atmospheric aerosols, plays an important role in the radiative balance of the earth system by directly heating the lower atmosphere and affecting the cloud cover through semi-indirect effects (Ramanathan and Carmichael, 2008). Although BC is hydrophobic, it can also act as a cloud condensation nucleus when internally mixed with other hydrophilic components (Zhang et al., 2008), indirectly affecting the radiative budget (Ramanathan et al., 2001). As a result, BC aerosols have a great impact on the regional/global climate and weather (Menon et al., 2002; Ramanathan and Carmichael, 2008; Ding et al., 2013; Liao et al., 2015; Huang et al., 2016). Recent research has also illustrated that BC increases atmospheric stability by its heating effect in the lower troposphere and cooling role at the surface (Wang et al., 2013). It suppresses the diffusion of pollutants, which deteriorates the air quality and plays an enhanced role in severe haze (Ding et al., 2016). However, it is difficult to accurately quantify the radiative forcing and environmental effects induced by BC because of the high variations in its concentration and physicochemical properties (IPCC, 2013). The light absorption of BC highly depends on its size and morphology. Mie calculations for hypothetical BC spheres show that the mass absorption cross-sections reach their peak at a diameter of ~150 nm and then decrease sharply with further increases in size (see Fig. 4 in Bond and Bergstrom, 2006). However, atmospheric BC particles apparently consist of aggregates of small primary spherules ~15 to 60 nm in diameter (Alexander et al., 2008; Zhang et al., 2008). They are chain agglomerates when freshly emitted from the combustion sources resulting in increasing mass normalized absorption with the particle mobility size (Khalizov et al., 2009). These fresh BC particles are quickly coated by other aerosol components in the atmosphere, leading to the collapse of the chain agglomerates into more compact BC cores (Zhang et al., 2008). An alteration in the morphology of BC due to a thin coating causes competition between light absorption enhancement and decline, resulting in little variation in the absorption efficiency (Wang et al., 2013; Peng et al., 2016). Subsequently, the thickened coating of the scattering shell enwrapping the compact BC cores enhances the light absorption of BC by the lensing effect, although the upper limit

Atmos. Chem. Phys. Discuss., doi:10.5194/acp-2016-1096, 2016
Manuscript under review for journal Atmos. Chem. Phys.
Published: 6 December 2016

Atmospheric Chemistry and Physics Discussions

of the enhanced amplitude varied among different studies (e.g., Schnaiter et al., 2005; Shiraiwa et al., 2010; Khalizov et al., 2009; Peng et al., 2016).

With the rapid development of its economy, China is suffering from heavy air pollution (Yin et al., 2016). As one of the major aerosol components, the annual BC emissions to the atmosphere are very high in China, representing approximately half of the emissions in Asia and one-fifth of the global BC emissions (Qin and Xie, 2012). The mass concentrations of BC have been widely measured (e.g., Cao et al., 2007; Zhang et al., 2008), but there is a lack of a comprehensive investigation of the physicochemical properties of ambient BC aerosols (e.g., size, morphology, and mixing state), due to the limitations of the measurement methodology. A traditional approach through analyzing the BC mass of size-segregated aerosol samples has usually been employed to determine the BC size distribution (Huang and Yu, 2008; Yu et al., 2010). However, it provides size information on the BC-containing particles rather than on the BC itself because numerous BC particles are internally mixed with other aerosol components in the ambient atmosphere (Shiraiwa et al., 2007; Schwarz et al., 2008). Additionally, the time resolutions of the determined BC size on the basis of this method are typically hours to days. In the last ten years, a novel analyzer–single particle soot photometer (SP2)–has provided an advantage to investigate in a highly time resolved manner of the mass and size of the refractory BC (rBC) (Stephens et al., 2003; Schwarz et al., 2006). The mixing state of rBC particles can also be derived from the measurement of SP2 (Gao et al., 2007; Moteki and Kondo, 2007, 2008; Laborde et al., 2012). Research on the sizes and mixing states of rBC based on this technology has been limited to a few regions in China (e.g., Huang et al., 2012; Wang et al., 2014a, 2015a; Wu et al., 2016; Gong et al., 2016), as the SP2 is very expensive and its performance is limited (Gysel et al., 2012; Liggio et al., 2012). It should be noted that the sizes of rBC reported by SP2 are generally mass-equivalent diameters rather than mobility- or aerodynamic-based ones, which are determined on the basis of the mass measurements of individual rBC-containing particles. Thus, they are independent of the morphology or mixing.

Although physicochemical properties of BC in the atmosphere are greatly diverse, its mass-equivalent sizes should vary little during their typical lifetime in the atmosphere

Atmos. Chem. Phys. Discuss., doi:10.5194/acp-2016-1096, 2016
Manuscript under review for journal Atmos. Chem. Phys.
Published: 6 December 2016

Atmospheric Chemistry and Physics Discussions

(~1 week) since BC itself is chemically inert under ambient conditions. In other words, the mass-size of a BC particle is independent of its morphology and mixing state, although coating with other components will reduce its mobility diameter and enlarge the size of the mixed particle in which the BC is embedded. As it is a byproduct of the incomplete combustion of fossil fuels and biomass, the BC size should be highly dependent on the emission sources, including fuel type and combustion condition. Based on the measurement of SP2, Liu et al. (2014) showed smaller sizes of the rBC cores from traffic than those from solid fuel sources and attributed the rBC concentrations from the two dominant sources accordingly. The rBC sizes measured at rural or remote sites were considerably larger than those measured at urban sites (Huang et al., 2012; Schwarz et al., 2013), implying that smaller sizes of rBC are emitted from traffic sources. Combining the measurement of SP2 and the chemical source apportionment of daily $PM_{2.5}$ samples, Wang et al. (2016) showed that the rBC from biomass burning and coal combustion had larger mass-equivalent diameter than that from traffic.

Jointly influenced by the local emissions (e.g., traffic exhaust) and regional transport of air pollutants from the surrounding heavily polluted areas where intense industrial emissions and coal combustions were reported, the source apportionments of $PM_{2.5}$ and its subcomponents (e.g., BC) in urban Beijing are highly controversial (Tao et al., 2016; Zíková et al., 2016). In this study, a novel approach was employed to evaluate the contribution of local traffic to the rBC concentration in urban Beijing during a wintertime in 2014 when hazes occurred frequently, on the basis of measurements of SP2 and reasonable assumptions. Before that, the mass-equivalent size distribution of rBC in urban Beijing was revealed. The variation in the rBC size was also investigated, accompanied by an analysis of their chemical compositions and potential source contributions.

2 Methodology

In situ measurements of rBC were conducted using a SP2 (Droplet Measurement Technology, Inc., Boulder, CO, USA) on the rooftop (approximately 8 m above ground

Atmos. Chem. Phys. Discuss., doi:10.5194/acp-2016-1096, 2016
Manuscript under review for journal Atmos. Chem. Phys.
Published: 6 December 2016

Atmospheric Chemistry and Physics Discussions

level) of an experimental building at the Tower Division of the Institute of Atmospheric Physics, Chinese Academy of Sciences (IAP, CAS), during a late winter period from 24 February to 15 March 2014, before the residential heating was stopped. The SP2 directly detects the incandescent intensity of an individual rBC-containing particle when it passes through an intra-cavity Nd:YAG laser beam with a Gaussian distribution (Schwarz et al., 2006). The incandescent intensity is converted to the mass of rBC based on the calibration of incandescent signals of size-selected soot standards performed pre/post-sampling. In this study, the Aquadag (Acheson, Inc., USA) was used as a reference rBC and size-selected by a scanning mobility particle sizer spectrometer (SMPS; TSI, Inc., Shoreview, MN, USA) for calibration. Compared to the ambient rBC, it is more sensitive to the incandescence signal. Thus, a scaling factor of 0.75 is employed with the calibration curve to induce more reliable rBC mass determinations (Baumgardner et al., 2012; Laborde et al., 2012). Moreover, an approximately 10% underestimation of the SP2-derived bulk rBC mass concentration due to the detection limitations outside the rBC mass range of ~0.3–120 fg was considered (Wang et al., 2014a, 2015a). The total uncertainty in the rBC mass determination was ~25%, including the uncertainties inherent in the mass calibration, flow measurement and estimation of BC masses beyond the SP2 detection range (Wu et al., 2016). The scattering signal is synchronously detected by the SP2 and used to determine the optical size of a single particle (Gao et al., 2007; Laborde et al., 2012). In this study, the scattering signal was employed to distinguish the mixing state of rBC-containing particles. A traditional method based on the delay time between the incandescent and scattering peaks was utilized to distinguish the rBC cores with and without a thick coating (Schwarz et al., 2006; Moteki and Kondo, 2007; Wang et al., 2014a; Wu et al., 2016). On this basis, the number fraction of thickly coated rBC (NF_{coated}), defined as the ratio of the number of thickly-coated rBC particles to that of all detectable rBC particles, was calculated to characterize the relative mixing extent of the BC aerosols in different ambient samples. A similar measurement was conducted in January 2013, and more details of the experimental setup and data process can be found in Wu et al. (2016).

Atmos. Chem. Phys. Discuss., doi:10.5194/acp-2016-1096, 2016
Manuscript under review for journal Atmos. Chem. Phys.
Published: 6 December 2016

Atmospheric Chemistry and Physics Discussions

Samples of $PM_{2.5}$ was collected twice a day during this campaign, with each lasting for twelve hours. The chemical contents including organic carbon (OC), elemental carbon (EC), water-soluble ions (e.g., SO_4^{2-}, NO_3^-, and NH_4^+) and trace elements were analyzed in the laboratory, as presented in detail by Lin et al. (2016).

3 Results and Discussion

3.1 Size distribution of rBC and its variation

As shown in Fig. 1, the mass of rBC ($dM/d\log D_p$) exhibits an approximately lognormal distribution as a function of the volume-equivalent diameter (*VED*) of void-free rBC, as has been commonly observed (e.g., Schwarz et al., 2006; Huang et al., 2012; Wang et al., 2016). A minor mode is also captured at large sizes (peaked at ~600 nm), only accounting for ~6% of the SP2-determined rBC masses. An analogous minor mode was previously observed at other sites in China. Huang et al. (2011) reported a minor peak with a diameter of ~690 nm at Kaiping, a rural site in the PRD region of China. Wang et al. (2014b) found a minor peak with a diameter of ~470–500 nm in a remote area of the Qinghai–Tibetan Plateau and considered that it was likely a feature of the rBC distribution of biofuel/open fire burning sources, which needs further measurements focusing on the size distribution at the emission sources. The peak diameter of the primary mode, with a value of 213 nm, during the campaign is well within the range (~150–230 nm) presented by previous studies conducted in different regions (Huang et al., 2012 and references therein). It should be noted that the density of the assumed void-free rBC was set to 1.8 g cm^{-3} in calculating the *VED* from the rBC masses measured in this study, which should result in larger *VED* values compared to those based on the density of 2.0 g cm^{-3} used in previous studies. If the same density with a value of 2.0 g cm^{-3} was employed, the peak diameter of the primary mode should be ~206 nm in this study. This value is very close to those observed in urban areas throughout China, e.g., 210 nm in Shenzhen in South China (Huang et al., 2012), 205 nm in Xi'an in West China (Wang et al., 2015b) and ~200 nm in Shanghai in East China (Gong et al., 2016). The relatively close mass-size distributions of rBC suggest that there are similar dominant emission sources in different urban regions in China, where

Atmos. Chem. Phys. Discuss., doi:10.5194/acp-2016-1096, 2016
Manuscript under review for journal Atmos. Chem. Phys.
Published: 6 December 2016

Atmospheric Chemistry and Physics Discussions

vehicle exhaust is one of the important sources emitting rBC particles. Compared to those measured at rural sites in the PRD region in South China (e.g., 220–222 nm, Huang et al., 2011, 2012), the peak diameters of rBC in urban areas are significantly lower. This might relate to the greater amounts of coal combustion and biomass burning around the rural sites (Huang et al., 2012). In contrast, the sizes of the rBC were much smaller in remote regions, e.g., with a peak diameter of ~175–188 nm in the Qinghai–Tibetan Plateau area (Wang et al., 2014b, 2015a). Wang et al. (2015a) attributed this lower peak diameter value to the source and considered that biomass burning generated a small rBC with peak *VED* values in the range of ~187–193 nm. Another important reason for the smaller rBC measured in remote regions, in our opinion, is that more large rBC particles are deposited during their long-range transport to the observation site. Further research on the sizes of rBC from different sources is needed.

The mass-size distributions of rBC during a polluted day (25 February) and a clean one (4 March) are also compared in Fig. 1. The average mass concentrations of rBC (MC_{rBC}) were 7.6 μg m^{-3} and 0.4 μg m^{-3}, respectively, on the polluted and clean days. The size distribution of rBC during the polluted day is similar to that during the entire observation period, although a larger peak diameter was observed, with a value of 221 nm. In contrast, the peak diameter on the clean day is much smaller, with a value of 199 nm. The secondary mode cannot be well characterized on the clean day. As mentioned above, the mass-sizes of rBC emitted from a certain source change little during their lifetime in the atmosphere. Thus, the considerable discrepancy of the rBC sizes illustrates significant source alteration during the polluted period compared to that on a clean day. Sun et al. (2014) used the measurements of ACSM at an urban site in Beijing to show that the regional contribution to the BC exceeded 50% during heavily polluted periods in January 2013. Model simulation also revealed that regional transport contributed an average of 56% to the $PM_{2.5}$ in Beijing in January 2013 when the hazes occurred frequently, and even higher during polluted periods (Li and Han, 2016). Accordingly, regional transport might play an important role in the increase in rBC sizes during polluted periods in urban Beijing. By comparison, traffic emissions should be the dominant source of rBC on the clean day, contributing to smaller rBC sizes.

Atmos. Chem. Phys. Discuss., doi:10.5194/acp-2016-1096, 2016
Manuscript under review for journal Atmos. Chem. Phys.
Published: 6 December 2016

Atmospheric Chemistry and Physics Discussions

The variation in the *VED* of the rBC is further investigated by comparing the mean *VED* value of rBC (VED_{rBC}) with the mass ratios of secondary inorganic components (i.e., ammonium sulfate, AS; ammonium nitrite, AN) to EC, a representation of the aerosol aging degree. Generally, the average VED_{rBC} of each sample shows an increasing trend, with increasing ratios of AS to EC (AS/EC) and AN to EC (AN/EC) with correlation coefficients of 0.63 ($p<0.01$) and 0.61 ($p<0.01$), respectively (Fig. 2a and 2b). Higher AS/EC and AN/EC values were observed in polluted samples, corresponding to a higher VED_{rBC} during these periods.

It is interesting to note that the VED_{rBC} correlates more closely with AS/EC than AN/EC, especially under a certain pollution level. For instance, the correlation coefficient between VED_{rBC} and AS/EC is 0.88 ($p<0.01$) during clean periods with a $PM_{2.5}$ mass concentration lower than 35 μg m^{-3} (blue dots in Fig. 2), much higher than that between VED_{rBC} and AN/EC. By contrast, the NF_{coated} varied less with AS/EC during these periods (Fig. 2c). This means that a higher AS/EC had less effect on the fraction of thickly coated rBC during these clean periods but was related to larger rBC sizes, which were highly dependent on the emission sources. In other words, higher AS/EC values might indicate an increasing contribution of sources other than traffic to rBC, as sulfur is one of the major trace elements of coal combustion but not of traffic (Zhang et al., 2013; Wang et al., 2016), corresponding to larger rBC sizes. On the other hand, NF_{coated} is highly related to AN/EC, with a correlation coefficient of 0.81 ($p<0.01$) during the clean periods (Fig. 2d). Even for the entire samples, the correlation coefficient between NF_{coated} and AN/EC can be as high as 0.81 ($p<0.01$), much higher than that between NF_{coated} and AS/EC, with a value of 0.65 ($p<0.01$). This implies that the mixing state of rBC is more sensitive to AN/EC in urban Beijing, especially during the clean periods. The secondary formation of AN might play an important role in the coating processes of rBC but have a smaller effect on the core size of the rBC.

3.2 Potential source contribution to rBC mass and size

The potential source contribution function (PSCF) based on hourly resolved 48-h backward trajectories arriving at the observation site 100 m above ground level were

Atmos. Chem. Phys. Discuss., doi:10.5194/acp-2016-1096, 2016
Manuscript under review for journal Atmos. Chem. Phys.
Published: 6 December 2016

Atmospheric Chemistry and Physics Discussions

257 performed using TrajStat software (Wang et al., 2009). The threshold of the PSCF
258 analysis was set to the mean value of each variable. A weight function on the gridded
259 PSCF values was employed on those cells having few trajectory endpoints (Wang et al.,
260 2006). Generally, the areas east and south of the observation site had the largest number
261 of potential source regions of high rBC concentrations, with weighted PSCF (WPSCF)
262 values of MC_{rBC} larger than 0.7 (Fig. 3a). Previous studies showed that Hebei province,
263 on the southern and eastern borders Beijing, was a major contributor of pollutants to
264 Beijing, as its industrial activities are intense (Zhang et al., 2013). The high coal
265 consumption associated with the heavy industrial activity and residential heating in the
266 cold season should be an important source of high atmospheric rBC loading in these
267 areas. Similarly, the distribution of the WPSCF values of VED_{rBC} shows that the eastern
268 and southern regions are also correlated with large VED_{rBC} values (Fig. 3b). This
269 implies that the pollution sources in these regions, e.g. heavy industrial activity and
270 residential heating, tend to produce highly concentrated rBC-containing particles with
271 large rBC core sizes. The source apportionment of rBC aerosols in London based on in
272 situ SP2 measurements showed that rBC-containing particles from solid fuel sources
273 (coal combustion and biomass burning) had significantly larger rBC cores than those
274 from traffic. Thus, the high WPSCF values of MC_{rBC} and VED_{rBC} in the east and south
275 might highly correlate to anthropogenic coal/biomass combustion in these regions.
276 The spatial distribution of the WPSCF values of NF_{coated} is shown in Fig. 3c. Associated
277 with the aging processes that increase the thickly coating states of rBC-containing
278 particles through heterogeneous reactions, the WPSCF values of NF_{coated} are generally
279 high in the areas surrounding the observation site. It should be noted that higher WPSCF
280 values of NF_{coated} (> 0.7) dominate in the east to south. In addition to the transport of
281 thickly coated BC particles from these regions, aging processes of locally emitted BC
282 particles (e.g., from traffic sources) under the southerly dominant condition, in which
283 the relative humidity (RH) is high (Zhang et al., 2015; Zheng et al., 2015), also increase
284 the fraction of thickly coated rBC (Wu et al., 2016). Although northerly/northwesterly
285 winds also blow aged rBC-containing particles with thick coatings, the larger amounts
286 of non-/thinly coated BC particles from local sources during these periods diminished

Atmos. Chem. Phys. Discuss., doi:10.5194/acp-2016-1096, 2016
Manuscript under review for journal Atmos. Chem. Phys.
Published: 6 December 2016

the WPSCF values of NF_{coated} in the north to west directions. The low RH and strong winds from these directions are unfavorable to the coating processes of locally emitted fresh rBC particles.

The VED_{coated}, defined as the *VED* of those thickly coated rBC cores, shows a dispersive WPSCF distribution (Fig. 3d). Compared to the distribution of VED_{rBC} with high WPSCF values that dominate in the east to south, high WPSCF values of VED_{coated} are located in the northern pathway of air masses being transported to the observation site as well. This implies that the regional transport of air masses brings large rBC, no matter which direction it comes from. Dominated by the locally emitted small rBC, the WPSCF values of VED_{rBC} are low in the northern region. It further illuminates that local sources such as traffic emit small rBC, while regional transport brings large rBC. On the basis of the large discrepancy in rBC sizes from local traffic against regional transport, it is possible to extract the contribution of local traffic emissions from the mixed rBC sources.

4 Discussion

4.1 Relationship between rBC size and mixing state

As large rBC sizes are usually accompanied by significant contributions of regional transport, which also lead to a high fraction of thickly coated rBC, the VED_{rBC} is directly compared with the NF_{coated} as shown in Fig. 4. The two-dimensional histogram of the 5-min average VED_{rBC} and NF_{coated} presents a significant linear correlation between the two variables. It is characterized more clearly by the variation in the mean VED_{rBC} values averaged in increased NF_{coated} bins with a resolution of 2% (magenta circles in Fig. 4). The observed minimum value of the 5-min NF_{coated} is ~10%, representing that there is little completely external mixing of rBC in the ambient atmosphere, even for short periods. However, an assumed mean *VED* of completely externally mixed rBC is extrapolated from the linear curve to NF_{coated} with a value of 0% (i.e., the *y*-intercept value). This inferred *VED*, with a value of ~150 nm, might be considered as the typical mean *VED* of freshly emitted rBC from vehicle exhaust, which is little coated (Zhang et al., 2008; Peng et al., 2016). We are surprised to find that the linear relationship

Atmos. Chem. Phys. Discuss., doi:10.5194/acp-2016-1096, 2016
Manuscript under review for journal Atmos. Chem. Phys.
Published: 6 December 2016

Atmospheric Chemistry and Physics Discussions

between VED_{rBC} and NF_{coated} seems to be common, as indicated by an almost identical result observed in another campaign conducted in January 2013 (Wu et al., 2016) (gray circles in Fig. 4). More observations are needed to verify this relationship. However, according to the results presented in this study, a mean *VED* of ~150 nm is legitimately accepted as the typical SP2-determined mean *VED* of fresh rBC from local traffic sources. As mentioned above, the *VED* of certain rBC varies little once it is emitted to the atmosphere. Thus, the mean *VED* with a value of ~150 nm was employed in this study as the representative of the rBC size from local traffic.

The variation in VED_{coated} with NF_{coated} is also shown (magenta triangles in Fig. 4). It is interested to find that, compared to VED_{rBC}, VED_{coated} presents a fluctuant variation as NF_{coated} increases. The larger VED_{coated} at lower NF_{coated} is comprehensible because regionally transported large rBC dominates in the thickly coated rBC particles, and the small rBC from local traffic is mainly externally mixed with other aerosol components at this stage. As the NF_{coated} increases from 10–20% to 30–40%, the mean VED_{coated} gradually decreases from ~200 nm to ~190 nm. This implies that some small rBC (e.g., rBC from local traffic) contributes a considerable part of the thickly coated rBC particles at this stage. In addition to the influence of the emission sources on the rBC size, this decrease in VED_{coated} can also be explained by the contamination of the local traffic emitted small rBC into the thickly coated rBC particles through atmospheric aging processes (i.e., coating with other components). It should be noted that the VED_{rBC} sustained increases at this stage, implying that other sources besides the local traffic also brought large rBC at the same time. This is because if the increase in NF_{coated} only results from the coating processes of the local traffic emitted rBC, the *VED* of the entire rBC (i.e., VED_{rBC}) should vary little. The VED_{coated} increases significantly when NF_{coated} exceeds 40%, suggesting that regional transport dominates at this stage, bringing a large amount of thickly coated rBC particles with a large rBC core. Meanwhile, the mean MC_{rBC} increases dramatically from 1.3 μg m^{-3} to 5.0 μg m^{-3} when NF_{coated} increases from 30% to 50%, further confirming the great contribution of regional transport to the rBC at this stage. By comparison, the mean rBC concentration varies less in the range of 0.8–1.4 μg m^{-3} when NF_{coated} is lower than 30%. The

Atmos. Chem. Phys. Discuss., doi:10.5194/acp-2016-1096, 2016
Manuscript under review for journal Atmos. Chem. Phys.
Published: 6 December 2016

observation from the campaign of 2013 shows a similar variation in VED_{coated} against NF_{coated} (gray triangles in Fig. 4).

4.2 Extracting the local traffic contribution to rBC

As VED_{rBC} with a value of ~150 nm is expected to be the typical mean *VED* of the local traffic emitted rBC and varies little in the atmosphere, it provides the possibility of extracting the contribution of the local traffic to the rBC from the total rBC mass concentration according to the variation in VED_{rBC}. However, the typical mean *VED* of rBC from other sources, such as coal combustion and biomass burning, is difficult to identify. It is dependent on many factors including fuel type and combustion condition. In this study, a simple assumption was employed to identify the typical mean *VED* of rBC from other sources besides local traffic according to where the air masses were from. During a short period when the source emissions are relatively stable, the rBC from a certain direction was assumed to have a certain mean *VED*, no matter from which source it is emitted. Thus, a cluster analysis was performed on the 48-h backward trajectories that arrived at the observation site. Five clusters were identified using TrajStat software according to the total spatial variation in the cluster numbers (as shown in Fig. S1). As the rBC tends to be more coated in the regionally transported air masses, the mean *VED* of the rBC from sources other than local traffic was derived from the values of VED_{coated}. The local traffic emitted small rBC also can also become thickly coated through aging processes in the atmosphere, so a further assumption is employed to consider the *VED* of rBC from other sources equal to the mean value of the upper 5% percentile of VED_{coated} in each cluster. Five typical mean *VED*s of rBC from sources other than local traffic were identified, with values in the range of 195.5–208.3 nm (Fig. S1). Such a simple assumption might have an impact on the absolute contribution of the local traffic to the rBC, but it should well reflect the variation in the traffic contribution.

Accordingly, the hourly-resolved traffic contribution to the rBC was extracted on the basis of the derived *VED* of the rBC from local traffic and other sources. The mass fraction of the traffic-induced rBC ($MF_{traffic}$) is shown in Fig. 5a (red line). During this

Atmos. Chem. Phys. Discuss., doi:10.5194/acp-2016-1096, 2016
Manuscript under review for journal Atmos. Chem. Phys.
Published: 6 December 2016

377 campaign, approximately 35% to 100% of the hourly MC_{rBC} is attributed to local traffic
378 emissions, with a mean of 59%. Based on a multiple linear regression analysis of the
379 contributions of the three dominant factors (i.e., traffic, coal combustion and biomass
380 burning) to the rBC derived from the chemical source apportionment of the daily $PM_{2.5}$
381 samples, Wang et al. (2016) showed a slightly lower contribution of the traffic to the
382 rBC in urban Xi'an, with a mean of 46% and a daily contribution in the range of 0.8 to
383 77.2%. Since entirely different methods were employed in addition to the different
384 locations, the resolved traffic contribution to the rBC should not be compared absolutely.
385 However, the relatively lower MC_{rBC} in this study (with a mean of 2.8 μg m^{-3} compared
386 to 8.0 μg m^{-3}) might partly interpret the slightly higher contribution of traffic, as a lower
387 MC_{rBC} is usually accompanied by a higher contribution of the local traffic. It is clear
388 that $MF_{traffic}$ is negatively correlated with MC_{rBC}, with the correlation coefficient as high
389 as -0.84 ($p<0.01$) between the daily moving averaged $MF_{traffic}$ and MC_{rBC} (Fig. 5a). This
390 means that the traffic contribution to the rBC decreased significantly during the polluted
391 periods when the rBC loading increased. In other words, the rBC from other sources
392 such as coal combustion and biomass burning play an increased role in these polluted
393 periods. This implies that the high MC_{rBC} in urban Beijing was not only due to the
394 accumulation of the local traffic emissions during stable synoptic conditions but also
395 be attributed to the overlaying pollution from other sources.
396 The diurnal variations of the decomposed MC_{rBC} from local traffic and other sources
397 are shown in Fig. 5b and 5c, respectively. A common diurnal variation in MC_{rBC} with
398 high values during the nighttime and low in the daytime is shown by both the traffic
399 and other sources producing rBC, suggesting the important impact of the mixing layer
400 height on the surface MC_{rBC}. A high mixing layer in the daytime, especially in the
401 afternoon, favors the diffusion of the pollutants, leading to a low value of MC_{rBC}. A low
402 mixing layer in the nighttime suppresses the diffusion of pollutants, resulting in a high
403 value of MC_{rBC}. It is noted that a significant peak MC_{rBC} of local traffic was observed
404 in the early morning (05:00–06:00 local time). Moreover, the increase in the local traffic
405 related MC_{rBC} occurs earlier than that of other sources in the evening. It corresponds
406 well to the increased traffic contribution in the morning and evening rush hours. To

Atmos. Chem. Phys. Discuss., doi:10.5194/acp-2016-1096, 2016
Manuscript under review for journal Atmos. Chem. Phys.
Published: 6 December 2016

Atmospheric Chemistry and Physics Discussions

some degree, the diurnal variation verifies the rationality of the method we employed to distinguish the contribution of the local traffic emission from that of other sources.

5 Summary and Concluding Remarks

An approximate lognormal size distribution of the rBC in volume-equivalent diameter in urban Beijing during a polluted wintertime in 2014 was observed on the basis of measurements using a SP2. The peak diameter was 213 nm, assuming void-free rBC with a density of 1.8 g cm^{-3}, which is close to the values observed in other urban areas in China. The measured sizes of the rBC were considerably larger during the polluted period than in the clean period, implying a source variation of the rBC. The mean VED_{rBC} was positively correlated with the ratios of secondary inorganic aerosols (including AS and AN) to EC, more significantly with AS/EC, especially at a certain pollution level. This implies that the rBC sizes are highly related to the emission sources because sulfur is one of the major trace elements in coal combustion, while little is emitted from traffic. By comparison, the mean NF_{coated} was correlated more with AN/EC, implying the important effect of the secondary formation of nitrate on the rBC mixing state. The PSCF analysis showed that regional transport from the east to south of Beijing was a major source of high rBC loading in Beijing and accompanied by a large VED_{rBC} and high NF_{coated}.

The relationship between VED_{rBC} and NF_{coated} was further discussed. A significant positive correlation existed among the two variables. The mean *VED* of the entire externally mixed rBC was extrapolated from the linear curve to NF_{coated} being equal to 0. The inferred *VED* with a value of 150 nm was considered as the typical mean *VED* of the rBC from local traffic. Based on the inferred *VED* and further reasonable assumptions, the local traffic contribution to the rBC was extracted using a multiple linear regression to VED_{rBC}. Traffic emissions played an important role in the rBC loading in urban Beijing, contributing 59% of the $MC_{rBC,}$ on average, in the campaign. However, its contribution decreased significantly in the polluted period. A significant negative correlation is found between the daily moving average MC_{rBC} and $MF_{traffic}$ with a coefficient of -0.87. A similar diurnal variation in the decomposed MC_{rBC}

Atmos. Chem. Phys. Discuss., doi:10.5194/acp-2016-1096, 2016
Manuscript under review for journal Atmos. Chem. Phys.
Published: 6 December 2016

Atmospheric Chemistry and Physics Discussions

437 associated with local traffic and other sources was observed with high values in the
438 nighttime and low in the daytime. However, a significant increase in traffic MC_{rBC} was
439 observed in the early morning and evening, indicating the increased contribution of
440 local traffic emissions. Although the absolute contribution of the local traffic might be
441 not entirely accurate in this study, as inferences and assumptions are employed, its
442 relative variation is still clear. Further research on the size measurement of rBC directly
443 from varied sources, including coal combustion, biomass burning and traffic exhaust,
444 is needed to validate our work. This work provides a relatively simple but novel method
445 to extract the contribution of the local traffic to the rBC on the basis of the size
446 measurement of the rBC in an ambient atmosphere. This work should be meaningful to
447 source apportionment research in urban Beijing where the air pollution is quite severe.
448
449 **Acknowledgments:**
450 This work was supported by the National Natural Science Foundation of China (No.
451 41575150, 41305128), the Special Scientific Research Funds for Environment
452 Protection Commonweal Section (No. 201409027) and the Jiangsu Collaborative
453 Innovation Center for Climate Change.
454

Atmos. Chem. Phys. Discuss., doi:10.5194/acp-2016-1096, 2016
Manuscript under review for journal Atmos. Chem. Phys.
Published: 6 December 2016

Atmospheric Chemistry and Physics Discussions

References:

Alexander, D. T. L., Crozier, P. A., and Anderson, J. R.: Brown carbon spheres in East Asian outflow and their optical properties, Sciences, 321, 833–836, 2008.

Baumgardner, D., Popovicheva, O., Allan, J., Bernardoni, V., Cao, J., Cavalli, F., Cozic, J., Diapouli, E., Eleftheiadis, K., Genberg, P. J., Gonzalez, C., Gysel, M., John, A., Kirchstetter, T. W., Kuhlbusch, T. A. J., Laborde, M., Lack, D., Müller, T., Niessner, R., Petzold, A., Piazzalunga, A., Putaud, J. P., Schwarz, J., Sheridan, P., Surramanian, R., Swietlicki, E., Valli, G., Vecchi, R., and Viana, M.: Soot reference materials for instrument calibration and intercomparisons: a workshop summary with recommendations, Atmos. Meas. Tech., 5, 1869–1887, 2012.

Bond, T. C., and Bergstrom, R. W.: Light absorption by carbonaceous particles: an investigative review, Aerosol Sci. Technol., 40, 27–67, 2006.

Cao, J. J., Lee, S. C., Chow, J. C., Watson, J. G., Ho, K. F., Zhang, R. J., Jin, Z. D., Shen, Z. X., Chen, G. C., Kang, Y. M., Zou, S. C., Zhang, L. Z., Qi, S. H., Dai, M. H., Cheng, Y., and Hu, K.: Spatial and seasonal distributions of carbonaceous aerosols over China, J. Geophys. Res., 112, D22S11, doi:10.1029/2006JD008205, 2007.

Ding, A. J., Fu, C. B., Yang, X. Q., Sun, J. N., Petäjä, T., Kerminen, V., Wang, T., Xie, Y. N., Herrmann, E., Zheng, L., Nie, W., Liu, Q., Wei X., and Kulmala, M.: Intense atmospheric pollution modifies weather: a case of mixed biomass burning wither fossil fuel combustion pollution in the eastern China, Atmos. Chem. Phys., 13, 10545-10554, 2013.

Ding, A. J., Huang, X., Nie, W., Sun, J. N., Kerminen, V.-M., Petäjä, T., Su, H., Cheng, Y. F., Yang, X.-Q., Wang, M. H., Chi, X. G., Wang, J. P., Virkkula, A., Guo, W. D., Yuan, J., Wang, S. Y., Zhang, R. J., Wu, Y. F., Song, Y., Zhu, T., Zilitinkevich, S., Kulmala, M., and Fu, C. B.: Enhanced haze pollution by black carbon in megacities in China, Geophys. Res. Lett., 43, 2873–2879, 2016.

Gao, R. S., Schwarz, J. P., Kelly, K. K., Fahey, D. W., Watts, L. A., Thompson, T. L., Spackman, J. R., Slowik, J. G., Cross, E. S., Han, J.-H., Davidovits, P., Onasch, T. B., and Worsnop, D. R.: A novel method for estimating light-scattering properties of soot aerosols using a modified single-particle soot photometer, Aerosol Sci. Technol., 41, 125–135, 2007.

Gong, X. D., Zhang, C., Chen, H., Nizkorodov, S. A., Chen, J. M., and Yang, X.: Size distribution and mixing state of black carbon particles during a heavy air pollution episode in Shanghai, Atmos. Chem. Phys., 16, 5399–5411, 2016.

Gysel, M., Laborde, M., Mensah, A., Corbin, J., Keller, A., Kim, J., Petzold, A., and Sierau, B.: Technical note: The single particle soot photometer fails to reliably detect PALAS soot nanoparticles, Atmos. Meas. Tech., 5, 3099–3107, 2012.

Huang, X., Ding, A. J., Liu, L. X., Liu, Q., Ding, K., Niu, X. R., Nie, W., Xu, Z., Chi, X. G., Wang, M. H., Sun, J. N., Guo, W. D., and Fu, C. B.: Effects of aerosol-radiation interaction on precipitation during biomass-burning season in East China, Atmos. Chem. Phys., 16, 10063–10082, 2016.

Huang, X. F., and Yu, J. Z.: Size distributions of elemental carbon in the atmosphere of a coastalurban area in South China: characteristics, evolution processes, and implications for the mixing state, Atmos. Chem. Phys., 8, 5843–5853, 2008.

Huang, X. F., Gao, R. S., Schwarz, J. P., He, L. Y., Fahey, D. W., Watts, L. A., McComiskey, A., Cooper, O. R., Sun, T. L., Zeng, L. W., Hu, M., and Zhang, Y. H.: Black carbon measurements in the Pearl River Delta region of China, J. Geophys. Res., 116, D12208,

doi:10.1029/2010JD014933, 2011.

Huang, X. F., Sun, T. L., Zeng, L. W., Yu, G. H., and Luan, S. J.: Black carbon aerosol characterization in a coastal city in South China using a single particle soot photometer, Atmos. Environ., 51, 21–28, 2012.

IPCC, 2013. Summary for policymakers. In: Stocker, T.F., Qin, D., Plattner, G.-K., Tignor, M., Allen, S.K., Boschung, J., Nauels, A., Xia, Y., Bex, V., Midgley, P.M. (Eds.), Climate Change 2013: The Physical Science Basis. Contribution of Working Group I to the Fifth Assessment Report of the Intergovernmental Panel on Climate Change. Cambridge University Press, Cambridge, United Kingdom and New York, NY, USA.

Khalizov, A. F., Xue, H. X., Wang, L., Zheng, J., and Zhang, R. Y.: Enhanced light absorption and scattering by carbon soot aerosol internally mixed with sulfuric acid, J. Phys. Chem. A, 113, 1066–1074, 2009.

Laborde, M., Mertes, P., Zieger, P., Dommen, J., Baltensperger, U., and Gysel, M.: Sensitivity of the single particle soot photometer to different black carbon types, Atmos. Meas. Tech., 5, 1031–1043, 2012.

Li, J. W., and Han, Z. W.: A modeling study of severe winter haze events in Beijing and its neighboring regions, Atmos. Res., 170, 87–97, 2016.

Liao, H., and Shang, J. J.: Regional warming by black carbon and tropospheric ozone: a review of progresses and research challenges in China, J. Meteor. Res., 29, 525–545, 2015.

Liggio, J. Gordon, M., Smallwood, G., Li, S.-M., Stroud, C., Staebler, R., Lu, G., Lee, P., Taylor, B., and Brook, J. R.: Are emissions of black carbon from gasoline vehicles underestimated? Insights from near and on-road measurements, Environ. Sci. Technol., 46, 4819–4828, 2012.

Lin, Y.-C., Hsu, S.-C., Chou, C.-C.-K., Zhang, R. J., Wu, Y. F., Kao, S.-J., Luo, L., Huang, C.-H., Lin, S.-H., and Huang, Y.-T.: Wintertime haze deterioration in Beijing by industrial pollution deduced from trace metal fingerprints and enhanced health risk by heavy metals, Environ. Pollut., 208, 284–293, 2016.

Liu, D., Allan, J. D., Young, D. E., Coe, H., Beddows, D., Fleming, Z. L., Flynn, M. J., Gallagher, M. W., Harrison, R. M., Lee, J., Prevot, A. S. H., Taylor, J. W., Yin, J., Williams, P. I., and Zotter, P.: Size distribution, mixing state and source apportionment of black carbon aerosol in London during wintertime, Atmos. Chem. Phys., 14, 10061–10084, 2014.

Menon, S., Hansen, J., Nazarenko, L., and Luo, Y. F.: Climate effects of black carbon aerosols in China and India, Science, 297, 2250–2253, 2002.

Moteki, N., and Kondo, Y.: Effects of mixing state on black carbon measurements by laser-induced incandescence, Aerosol Sci. Technol., 41, 398–417, 2007.

Moteki, N., and Kondo, Y.: Method to measure time-dependent scattering cross sections of particles evaporating in a laser beam, J. Aerosol Sci., 39, 348–364, 2008.

Peng, J. F., Hu, M., Guo, S., Du, Z. F., Zheng, J., Shang, D. J., Zamora, M. L., Zeng, L. M., Shao, M., Wu, Y.-S., Zheng, J., Wang, Y., Glen, C. R., Collins, D. R., Molina, M. J., and Zhang, R. Y.: Markedly enhanced absorption and direct radiative forcing of black carbon under polluted urban environments, Proc. Natl. Acad. Sci. U.S.A., 113, 4266–4271, 2016.

Qin, Y., and Xie, S. D.: Spatial and temporal variation of anthropogenic black carbon emissions in China for the period 1980–2009, Atmos. Chem. Phys., 12, 4825–4841, 2012.

Ramanathan, V., Crutzen, P. J., Kiehl, J. T., and Rosenfeld, D.: Aerosols, climate, and the hydrological cycle, Science, 294, 2119–2125, 2001.

543 Ramanathan, V., and Carmichael, G.: Global and regional climate changes due to black carbon,
544 Nature Geosci., 1, 221–227, 2008.
545 Schnaiter, M., Linke, C., Möhler, O., Naumann, K. H., Saathoff, H., Wagner, R., Schurath, U., and
546 Wehner, B.: Absorption amplification of black carbon internally mixed with secondary organic
547 aerosol, J. Geophys. Res., 110, D19204, doi:10.1029/2005JD006046, 2005.
548 Schwarz, J. P., Gao, R. S., Fahey, D. W., Thomson, D. S., Watts, L. A., Wilson, J. C., Reeves, J. M.,
549 Darbeheshti, M., Baumgardner, D. G., Kok, G. L., Chung, S. H., Schulz, M., Hendricks, J.,
550 Lauer, A., Kärcher, B., Slowik, J. G., Rosenlof, K. H., Thompson, T. L., Langford, A. Q.,
551 Loewenstein, M., and Aikin, K. C.: Single-particle measurements of midlatitude black carbon
552 and light-scattering aerosols from the boundary layer to the lower stratosphere, J. Geophys.
553 Res., 111, D16207, doi:10.1029/2006JD007076, 2006.
554 Schwarz, J. P., Gao, R. S., Spackman, J. R., Watts, L. A., Thomson, D. S., Fahey, D. W., Ryerson,
555 T. B., Peischl, J., Holloway, J. S., Trainer, M., Frost, G. J., Baynard, T., Lack, D. A., de Gouw,
556 J. A., Warneke, C., and Del Negro, L. A.: Measurement of the mixing state, mass, and optical
557 size of individual black carbon particles in urban and biomass burning emissions, Geophys.
558 Res. Lett., 35, L13810, doi:10.1029/2008GL033968, 2008.
559 Schwarz, J. P., Gao, R. S., Perring, A. E., Spackman, J. R., and Fahey, D. W.: Black carbon aerosol
560 size in snow, Sci. Rep., 3, 1356, doi:10.1038/srep01356, 2013.
561 Shiraiwa, M., Kondo, Y., Moteki, N., Takegawa, N., Miyazaki, Y., and Blake, D. R.: Evolution of
562 mixing state of black carbon in polluted air from Tokyo, Geophys. Res. Lett., 34, L16803,
563 doi:10.1029/2007GL029819, 2007.
564 Shiraiwa, M., Kondo, Y. Iwamoto, T., Kita, K.: Amplification of light absorption of black carbon by
565 organic coating, Aerosol Sci. Technol., 44, 46–54, 2010.
566 Stephens, M., Turner, N., and Sandberg, J.: Particle identification by laser-induced incandescence
567 in a solid-state laser cavity, Appl. Opt., 42, 3726–3736, 2003.
568 Sun, Y. L., Jiang, Q., Wang, Z. F., Fu, P. Q., Li, J., Yang, T., and Yin, Y.: Investigation of the sources
569 and evolution processes of severe haze pollution in Beijing in January 2013, J. Geophys. Res.
570 Atmos., 119, 4380–4398, 2014.
571 Tao, J., Zhang, L. M., Zhang, R. J., Wu, Y. F., Zhang, Z. S., Zhang, X. L., Tang, Y. X., Cao, J. J.,
572 and Zhang, Y. H.: Uncertainty assessment of source attribution of $PM_{2.5}$ and its water-soluble
573 organic carbon content using different biomass burning tracers in positive matrix factorization
574 analysis — a case study in Beijing, China, Sci. Total Environ., 543, 326–335, 2016.
575 Wang, Q. Y., Huang, R. J., Cao, J. J., Han, Y. M., Wang, G. H., Li, G. H., Wang, Y. C., Dai, W. T.,
576 Zhang, R. J., and Zhou, Y. Q.: Mixing state of black carbon aerosol in a heavily polluted urban
577 area of China: implications for light absorption enhancement, Aerosol Sci. Technol., 48, 689–
578 697, 2014a.
579 Wang, Q. Y., Schwarz, J. P., Cao, J. J., Gao, R. S., Fahey, D. W., Hu, T. F., Huang, R. J., Han, Y. M.,
580 and Shen, Z. X.: Black carbon aerosol characterization in a remote area of Qinghai–Tibetan
581 Plateau, western China, Sci. Total Environ., 479–480, 151–158, 2014b.
582 Wang, Q. Y., Huang, R. J., Cao, J. J., Tie, X. X., Ni, H. Y., Zhou, Y. Q., Han, Y. M., Hu, T. F., Zhu,
583 C. S., Feng, T., Li, N., and Li, J. D.: Black carbon aerosol in winter northeastern Qinghai–
584 Tibetan Plateau, China: the source, mixing state and optical property, Atmos. Chem. Phys., 15,
585 13059–13069, 2015a.
586 Wang, Q. Y., Liu, S. X., Zhou, Y. Q., Cao, J. J., Han, Y. M., Ni, H. Y., Zhang, N. N., and Huang, R.

J.: Characteristics of Black Carbon Aerosol during the Chinese Lunar Year and Weekdays in Xi'an, China, Atmosphere, 6, 195–208, 2015b.

Wang, Q. Y., Huang, R. J., Zhao, Z. Z., Cao, J. J., Ni, H. Y., Tie, X. X., Zhao, S. Y., Su, X. L., Han, Y. M., Shen, Z. X., Wang, Y. C., Zhang, N. N., Zhou, Y. Q., and Corbin, J. C.: Physicochemical characteristics of black carbon aerosol and its radiative impact in a polluted urban area of China, J. Geophys. Res. Atmos., 121, doi:10.1002/2016JD024748, 2016.

Wang, Y., Khalizov, A., Levy, M., and Zhang, R. Y.: New direction: light absorbing aerosols and their atmospheric impacts, Atmos. Environ., 81, 713–715, 2013.

Wang, Y. Q., Zhang, X. Y., and Arimoto, R.: The contribution from distant dust sources to the atmospheric particulate matter loadings at Xi'an, China during spring, Sci. Total Environ., 368, 875–883, 2006.

Wang, Y. Q., Zhang, X. Y., and Draxler, R. R.: TrajStat: GIS-based software that uses various trajectory statistical analysis methods to identify potential sources from long-term air pollution measurement data, Environ. Modell. Softw., 24, 938–939, 2009.

Wu, Y. F., Zhang, R. J., Tian, P., Tao, J., Hsu, S.-C., Yan, P., Wang, Q. Y., Cao, J. J., Zhang, X. L., and Xia, X. A.: Effect of ambient humidity on the light absorption amplification of black carbon in Beijing during January 2013, Atmos. Environ., 124, 217–223, 2016.

Yin, Z. C., and Wang, H. J.: Seasonal prediction of winter haze days in the north central North China Plain, Atmos. Chem. Phys., 16, 14843–14852, 2016.

Yu, H., Wu, C., Wu, D., and Yu, J. Z.: Size distributions of elemental carbon and its contribution to light extinction in urban and rural locations in the Pearl River Delta region, China, Atmos. Chem. Phys., 10, 5107–5119, 2010.

Zhang, Q., Quan, J. N., Tie, X. X., Li, X., Liu, Q., Gao, Y., and Zhao, D. L.: Effects of meteorology and secondary particle formation on visibility during heavy haze events in Beijing, China, Sci. Total Environ., 502, 578–584, 2015.

Zhang, R., Jing, J., Tao, J., Hsu, S.-C., Wang, G., Cao, J., Lee, C.S.L., Zhu, L., Chen, Z., Zhao, Y., and Shen, Z.: Chemical characterization and source apportionment of PM2.5 in Beijing: seasonal perspective, Atmos. Chem. Phys., 13, 7053–7074, 2013.

Zhang, R. Y., Khalizov, A. F., Pagels, J. Zhang, D., Xue, H. X., and McMurry, P. H.: Variability in morphology, hygroscopicity, and optical properties of soot aerosols during atmospheric processing, Proc. Natl. Acad. Sci. U.S.A., 105, 10291–10296, 2008.

Zhang, X. Y., Wang, Y. Q., Zhang, X., Guo, W., Gong, S. L.: Carbonaceous aerosol composition over various regions of China during 2006, J. Geophys. Res., 113, D14111, doi:10.1029/2007JD009525, 2008.

Zheng, G. J., Duan, F. K., Su, H., Ma, Y. L., Cheng, Y., Zheng, B., Zhang, Q., Huang, T., Kimoto, T., Chang, D., Pöschl., U., Cheng, Y. F., and He, K. B.: Exploring the severe winter haze in Beijing: the impact of synoptic weather, regional transport and heterogeneous reactions, Atmos. Chem. Phys., 15, 2969–2983, 2015.

Zíková, N., Wang, Y. G., Yang, F. M., Li, X. H., Tian, M., and Hopke, P. K.: On the source contribution to Beijing PM2.5 concentrations, Atmos. Environ., 134, 84–95, 2016.

Atmos. Chem. Phys. Discuss., doi:10.5194/acp-2016-1096, 2016
Manuscript under review for journal Atmos. Chem. Phys.
Published: 6 December 2016

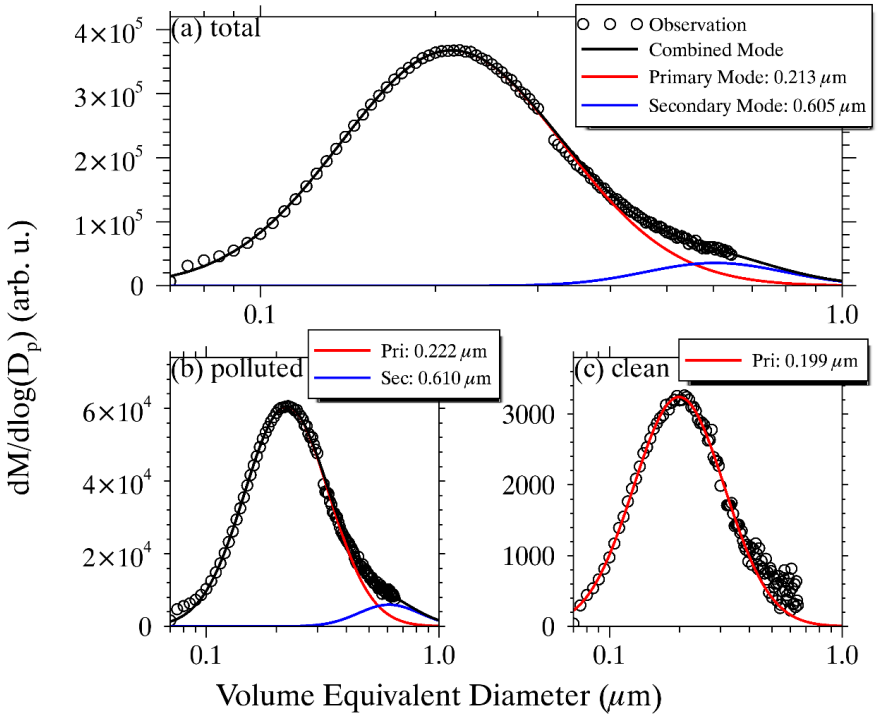

Fig. 1. Size distributions of rBC in volume-equivalent diameter during a campaign from 24 February to 15 March, 2014. The red and blue lines are the lognormal fittings to the primary and secondary modes, respectively, and the black ones correspond to the combined mode.

Atmos. Chem. Phys. Discuss., doi:10.5194/acp-2016-1096, 2016
Manuscript under review for journal Atmos. Chem. Phys.
Published: 6 December 2016

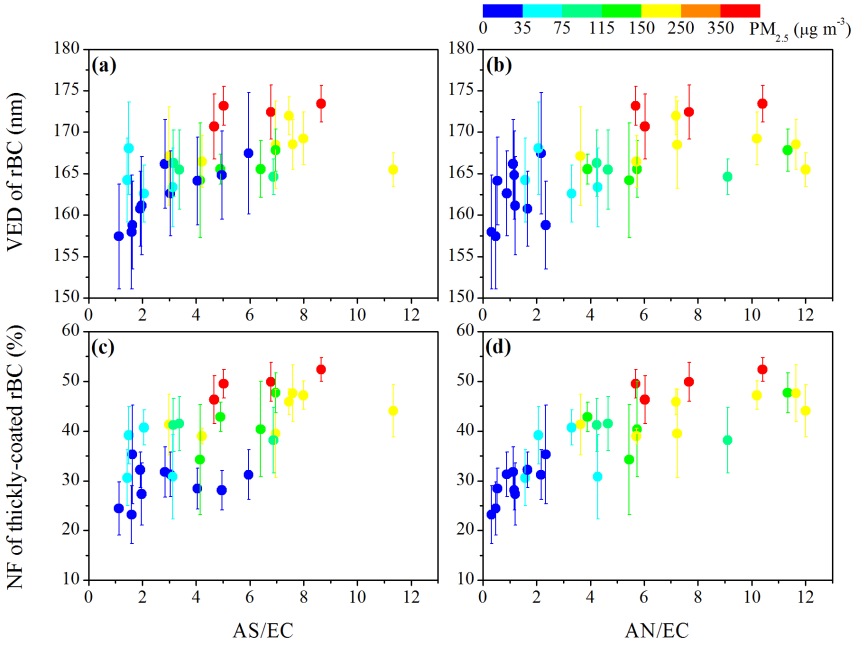

634

635 Fig. 2. Variation in the average volume-equivalent diameters of rBC (VED_{rBC}) as a function of the
636 mass ratios of (a) ammonium sulfate (AS) and (b) ammonium nitrite (AN) to elemental carbon (EC).
637 The same apply for (c) and (d), but for the number fraction of thickly coated rBC (NF_{coated}). The
638 vertical bar denotes one standard deviation. The color scale represents the pollution levels defined
639 as the $PM_{2.5}$ mass concentration according to the AQI standard of MEP of China.

640

Atmos. Chem. Phys. Discuss., doi:10.5194/acp-2016-1096, 2016
Manuscript under review for journal Atmos. Chem. Phys.
Published: 6 December 2016

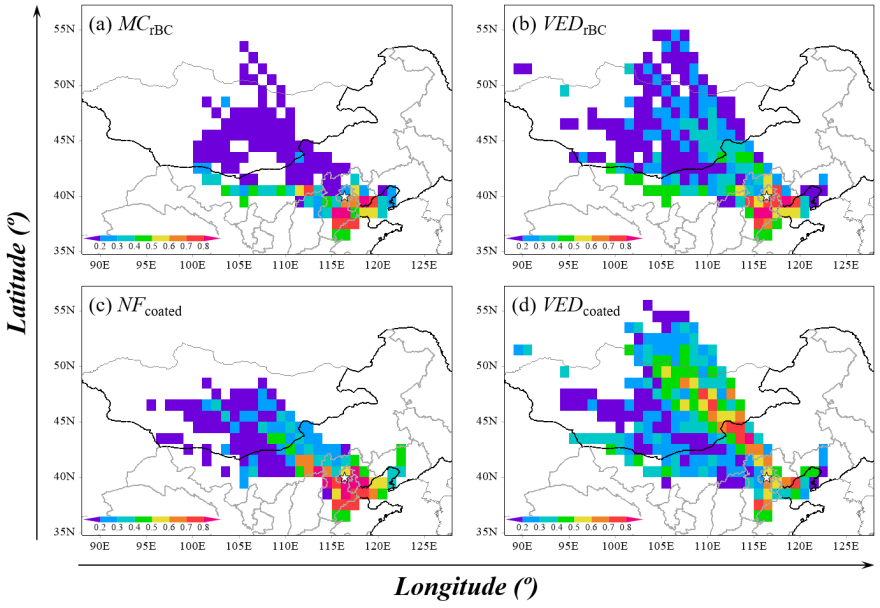

Fig. 3. Distributions of gridded (1°×1°) potential source contribution functions of (a) mass concentration (*MC*) and (b) volume equivalent diameter (*VED*) of rBC, and (c) number fraction (*NF*) and (d) *VED* of thickly coated rBC. The overlaid star symbol represents the geographical location of the observation site.

Atmos. Chem. Phys. Discuss., doi:10.5194/acp-2016-1096, 2016
Manuscript under review for journal Atmos. Chem. Phys.
Published: 6 December 2016

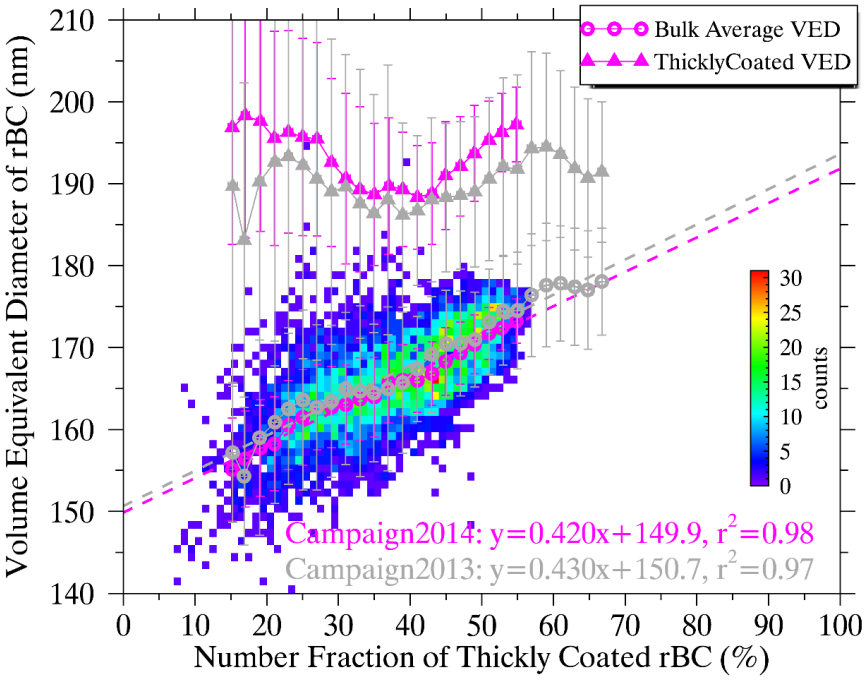

Fig. 4. Two-dimensional histogram of the 5-min average volume equivalent diameter of rBC (VED_{rBC}) against number fraction of thickly coated rBC (NF_{coated}) during the campaign in the late winter in 2014. The magenta circles and triangles with error bars represent the mean VED_{rBC} and VED of thickly-coated rBC (VED_{coated}) averaged in each NF_{coated} bin with a resolution of 2%, respectively. The dashed magenta line denotes the linear regression of VED_{rBC} against NF_{coated}. The relationship between VED_{rBC} and NF_{coated} during another campaign in January 2013 (Wu et al., 2016) is comparatively overlapped in gray.

Atmos. Chem. Phys. Discuss., doi:10.5194/acp-2016-1096, 2016
Manuscript under review for journal Atmos. Chem. Phys.
Published: 6 December 2016

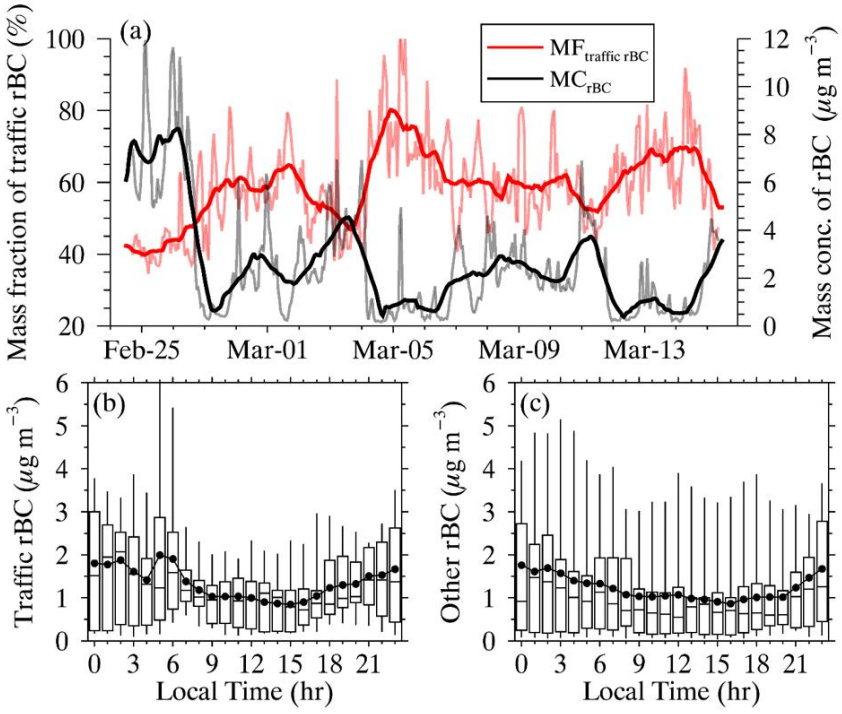

Fig. 5. (a) Time series of hourly mass concentration of rBC (MC_{rBC}) and mass fraction of local traffic related rBC ($MF_{traffic}$). The bold lines represent the variations of the daily moving averaged MC_{rBC} and $MF_{traffic}$. (b) and (c) show the diurnal variations in the decomposed rBC from local traffic emission and other sources, respectively.